*Inorg. Chem.* **2002**, *41*, 715–726


# Synthesis and Structural Studies of 1,1′-Bis-Amino-Functionalized Ferrocenes, Ferrocene Salts, and Ferrocenium Salts

**Sam Bradley, Kenneth D. Camm, Xiaoming Liu, Patrick C. McGowan,* Raheela Mumtaz, Karrie A. Oughton, Thomas J. Podesta, and Mark Thornton-Pett**

*School of Chemistry, University of Leeds, Leeds LS2 9JT, U.K.*

Received August 1, 2001

Having isolated and characterized a series of sodium cyclopentadienide salts, we have synthesized a number of 1,1′-bis-amino-functionalized ferrocenes, 1,1′-bis-amino-functionalized ferrocene salts, and 1,1′-bis-amino-functionalized ferrocenium salts. Among these are the first crystallographically characterized examples of cyclopentadienyl units containing (piperidin-*N*-ylethyl)- and (pyrid-2-ylmethyl)cyclopentadienyl side chains. In the cases of some of the ferrocenes, ferrocene salts, and ferrocenium salts, there are some interesting structural features in the solid state. These include C–H···N and C–H···$\pi$ cloud interactions as well as N–H···O and N–H···F hydrogen bonds.

## Introduction

Recently there has been much interest and research activity into the potent antitumor behavior of metallocenes such as titanocene dichloride, vanadocene dichloride, niobocene dichloride, and molybdocene dichloride.[1] Indeed we have published facile and high-yielding methods of synthesizing functionalized water-soluble and stable titanocenes, which are currently being evaluated as antitumor reagents.[2,3] We have also published other water-soluble organometallic systems.[4−6] There has also been antitumor activity reported for a number of ferrocenium compounds[7] as well as DNA binding studies of such compounds being carried out recently.[8] Other studies on functionalized ferrocenes and ferrocenium salts suggest that the cytotoxic behavior of ferrocenium salts is based on their ability to generate oxygen active species, which can damage DNA.[9] Another area of application in the biological arena is the observation that amino-functionalized derivatives of ferrocenyl-substituted quinoline compounds have been shown to have significantly higher antimalarial activity than chloroquinine, both in vivo and in vitro.[10] Functionalized ferrocenes have also been reported to act as anion receptors as evidenced using $^1$H NMR studies.[11]

Multidentate functionalized ferrocenes can also be prepared where there are more than two donor heteroatoms.[12] These, like many bisfunctionalized ferrocenes, start with ferrocene as the starting material, and quite often there are many steps to arrive at the end product. For example, until recently, the most successful way of preparing bis(dimethylamino)ferrocene is using a Mannich-type reaction, yielding the product in 17%. Progress has been made for one specific case of the improved preparation of 1,1′-bis[(*N*,*N*-dimethylamino)methyl]ferrocene by treatment of 1,1′-dilithioferrocene−TMEDA with Eschenmoser's salt *N*,*N*-dimethyleneammonium iodide, followed by purification of the product by chromatography.[13] Thus, finding easy and high-yielding synthetic routes to a variety of different ferrocenes and their salts is a desirable goal.

* To whom correspondence should be addressed. E-mail: p.c.mcgowan@chem.leeds.ac.uk.

(1) Yang, P.; Guo, M. *Coord. Chem. Rev.* **1999**, *185*, 189−211.
(2) McGowan, M. A. D.; McGowan, P. C. *Inorg. Chem. Commun.* **2000**, 337−341.
(3) McGowan, M. A. D.; McGowan, P. C. British Patent 0.99293553.2, 1999.
(4) McGowan, P. C.; Hart, C. E.; Donnadieu, B.; Poilblanc, R. *J. Organomet. Chem.* **1997**, *528*, 191−194.
(5) Philippopoulos, A. I.; Hadjiliadis, N.; Hart, C. E.; Donnadieu, B.; McGowan, P. C.; Poilblanc, R. *Inorg. Chem.* **1997**, *36*, 1842−1849.
(6) Bradley, S.; McGowan, P. C.; Oughton, K. A.; Thornton-Pett, M.; Walsh, M. E. *Chem. Commun.* **1999**, 77−79.
(7) Kopf-Maier, P.; Kopf, H.; Neuse, E. W. *Angew. Chem., Int. Ed. Engl.* **1994**, *23*, 446.
(8) Georgopoulou, A. S.; Mingos, D. M. P.; White, A. J. P.; Williams, D. J.; Horrocks, B. R.; Houlton, A. *J. Chem. Soc., Dalton Trans.* **2000**, 2969−2974.
(9) Osella, D.; Ferrali, M.; Zanello, P.; Laschi, F.; Fontani, M.; Vervi, C.; Caviglio, G. *Inorg. Chim. Acta* **2000**, *306*, 42.
(10) Biot, C.; Delhaes, L.; Abessolo, H.; Domarle, O.; Maciejewski, L. A.; Mortuaire, M.; Delcourt, P.; Deloron, P.; Camus, D.; Dive, D.; Brocard, J. S. *J. Organomet. Chem.* **1999**, *589*, 59−65.
(11) Beer, P. D. *Acc. Chem. Res.* **1998**, *31*, 71−80.
(12) Long, N. J.; Martin, J.; White, A. J. P.; Williams, D. J. *J. Chem. Soc., Dalton Trans.* **1997**, 3083−3085.
(13) Glidewell, C.; Royles, B. J. L.; Smith, D. M. *J. Organomet. Chem.* **1997**, *527*, 259−261.

10.1021/ic010821k CCC: $22.00 
Published on Web 01/25/2002

In this paper we report general and high-yielding routes to the preparation of amino-functionalized ferrocenes and their corresponding ferrocene and ferrocenium salts. We have been able to achieve this with different lengths of spacer with varying flexibility between the cyclopentadienyl ring and the amino functionality. Thus, a series of new compounds are presented, many of which have interesting intermolecular interactions. Part of this work has been previously communicated:[6] this paper gives a more detailed account including experimental details, characterization data, electrochemical data, and seven new crystal structures. Of particular significance are the first crystallographically characterized organometallic compounds with the ligand system of (piperidin-*N*-ylethyl)- and (pyrid-2-ylmethyl)-cyclopentadienyl side chains. Also of note is the synthesis of a series of novel amino-functionalized ferrocenium compounds. An excellent review of functionalized cyclopentadienyl compounds has been written by Jutzi.[14]

## Experimental Section

**General Procedures**. Standard inert atmosphere techniques were used throughout. Acetonitrile and dichloromethane were distilled from $CaH_2$. Petrol (40−60 °C), diethyl ether, toluene, and THF were distilled from $Na/Ph_2CO$. NMR solvents were degassed by three freeze−pump−thaw cycles and stored over 3 Å molecular sieves in a drybox. All reagents were purchased in reagent grade and used without further purification.

**Instrumentation**. $^1H$ and $^{13}C$ NMR spectra were recorded on Bruker 250, 300, and 500 MHz spectrometers. IR spectra were recorded on a Perkin-Elmer 1600 spectrometer. High-resolution mass spectrometry was performed by the University of Leeds mass spectral service. Elemental analyses were performed by the University of Leeds microanalytical services. Cyclic voltammetry was performed at room temperature in an appropriate solvent (see Table 10), using an Autolab PGSTAT 30 potentiostat driven by GPES 4.5 (Eco Chemie). A standard three-electrode system was used, a working electrode (0.5 mm diameter planar Pt disc), a 2 mm Pt rod counter electrode, and a Ag/AgCl/0.05 M $[N^nBu_4]Cl$, 0.45 M $[N^nBu_4][BF_4]$ in $CH_2Cl_2$ reference electrode. A 0.10 V scanning rate was used. Potentials were quoted against internal standard, ferrocenium/ferrocene couple. Throughout the measurements, IR compensation was applied using positive feedback.

**Fe{$\eta$-$C_5H_4(CH_2)_2NMe_2$}$_2$ (1)**. To a Schlenk tube charged with $FeCl_2$ (0.40 g, 0.003 mol) and THF (50 mL) was added a suspension of $NaC_5H_4(CH_2)_2NMe_2$ (1.0 g, 0.006 mol) in THF (30 mL) via cannula. The reaction mixture was stirred overnight. The solvent was removed in vacuo. The product was washed with toluene (2 × 30 mL). The extracts were combined, and removal of the solvent afforded the product as a viscous orange oil (0.8 g, 0.002 mol, 79%). Anal. Calcd for $FeC_{18}H_{28}N_2$: C, 65.8; H, 8.4; N, 8.5. Found: C, 65.5; H, 8.5; N, 8.3. $^1H$ NMR ($C_6D_6$, 250.1 MHz, 300 K): $\delta$ 3.91 [br s, 8H, $C_5H_4CH_2CH_2NMe_2$], 2.37 [m, 8H, $CH_2CH_2NMe_2$], 2.18 [s, 12H, $CH_2CH_2NMe_2$]. $^{13}C\{^1H\}$ NMR ($C_6D_6$, 62.9 MHz, 300 K): $\delta$ 86.7 [s, $C(CH_2)_2NMe_2$], 68.7, 67.9 [2 × s, CH of $C_5H_4(CH_2)_2NMe_2$], 61.1 [s, $CH_2NMe_2$)], 45.5 [s, $C_5H_4(CH_2)_2NMe_2$], 27.8 [s, $CH_2CH_2NMe_2$]

**Fe{$\eta$-$C_5H_4(CH_2)_3NMe_2$}$_2$ (2)**. To a Schlenk tube charged with $FeCl_2$ (0.55 g, 0.004 mol) and THF (50 mL) was added a suspension of $NaC_5H_4(CH_2)_2NMe_2$ (1.5 g, 0.009 mol) in THF (50 mL) via cannula. The reaction mixture was stirred overnight. The solvent was removed in vacuo. The product was extracted with toluene (2 × 30 mL). The extracts were combined, and removal of the solvent afforded the product as a viscous orange oil (1.0 g, 0.003 mol, 66%). FAB MS: *m*/*z* 328, $Fe[Cp(CH_2)_3NMe_2]_2$. $^1H$ NMR ($C_6D_6$, 250.1 MHz, 300 K): $\delta$ 3.97 [br s, 8H, $C_5H_4CH_2CH_2CH_2NMe_2$], 2.50−2.30 [m, 8H $CH_2CH_2CH_2NMe_2$], 2.23 [s, 12H, $CH_2CH_2CH_2NMe_2$], 1.66 [m, 4H, $CH_2CH_2CH_2NMe_2$]. $^{13}C\{^1H\}$ NMR ($C_6D_6$, 62.9 MHz, 300 K): $\delta$ 88.8 [s, $C(CH_2)_3NMe_2$], 68.6, 67.8 [2 × s, CH of $C_5H_4(CH_2)_3NMe_2$], 59.6 [s, $CH_2CH_2CH_2NMe_2$], 45.4 [s, $CH_2CH_2CH_2NMe_2$], 29.2, 27.2 [2 × s, $CH_2CH_2CH_2NMe_2$].

**Fe{$\eta$-$C_5H_4CH(CH_2)_4NMe$}$_2$ (3)**. To a Schlenk tube charged with $FeCl_2$ (1.0 g, 0.008 mol) and THF (50 mL) was added a suspension of $NaC_5H_4CH(CH_2)_4NMe$ (2.9 g, 0.016 mol) in THF (30 mL) via cannula. The reaction mixture was stirred overnight. The solution was removed by filtration and the solid washed with toluene (2 × 50 mL). The volatiles were removed from the combined filtrate and washings in vacuo. The product was recrystallized from petroleum ether (bp 40−60 °C) to afford the product as a bright yellow, orange solid (1.9 g, 0.005 mol, 63%.) Anal. Calcd for $FeC_{20}H_{32}N_2$: C, 69.5; H, 7.4; N, 8.5. Found: C, 69.2; H, 7.3; N, 8.2. $^1H$ NMR ($C_6D_6$, 250.1 MHz, 300 K): $\delta$ 3.97 [s, 8H, $C_5H_4CH(CH_2CH_2)_2NMe$], 2.80 [m, 4H, $CH(CH_2CH_{2\,ax})_2NMe$], 2.19 [s, 6H, $CH(CH_2CH_2)_2NMe$] , 2.19 [t of t, 2H, $CH(CH_2CH_2)_2NMe$], 1.97−1.15 [m, 12H, $CH(CH_2CH_{2eq})_2NMe$]. $^{13}C\{^1H\}$ NMR ($C_6D_6$, 62.9 MHz, 300 K): $\delta$ 94.9 [s, $CCH(CH_2CH_2)_2NMe$], 68.3, 67.0 [2 × s, CH of $C_5H_4CH(CH_2CH_2)_2NMe$], 56.9 [s, $CH(CH_2CH_2)_2NMe$], 47.0 [s, $CH(CH_2CH_2)_2NMe$], 35.9 [s, CH of $CH(CH_2CH_2)_2NMe$], 33.6 [s, $CH_2$ of $(CH_2CH_2)_2NMe$].

**Fe{$\eta$-$C_5H_4(CH_2)_2N(CH_2)_5$}$_2$ (4)**. To a Schlenk tube charged with $FeCl_2$ (0.5 g, 0.004 mol) and THF (50 mL) was added a suspension of $NaC_5H_4(CH_2)_2N(CH_2)_5$ (1.57 g, 0.008 mol) in THF (30 mL) via cannula. The reaction mixture was stirred overnight. The solution was decanted, and the solvent was removed in vacuo. The product was washed with petroleum ether (bp 40−60 °C) and extracted with toluene (30 mL). Toluene was removed in vacuo to give an orange-yellow solid. Recrystallization from diethyl ether afforded yellow crystalline needles (1.4 g, 0.003 mol, 85%). FAB MS: *m*/*z* 409, $Fe\{C_5H_4(CH_2)_2N(CH_2)_5\}_2$. $^1H$ NMR ($C_6D_6$, 250.1 MHz, 300 K): $\delta$ 4.02, 3.98 [2 × virt t, 8H, $C_5H_4(CH_2)_2N(CH_2)_5$], 2.55 [m, 4H, $CH_2CH_2N(CH_2)_5$], 2.38 [m, 8H, $(CH_2)_2N(CH_2)_2(CH_2)_2(CH_2)$], 1.55 [m, 8H, $(CH_2)_2N(CH_2)_2(CH_2)_2(CH_2)$], 1.37 [m, 4H, $(CH_2)_2N(CH_2)_2(CH_2)_2(CH_2)$]. $^{13}C\{^1H\}$ NMR ($C_6D_6$, 62.9 MHz, 300 K): $\delta$ 87.9 [s, $C(CH_2)_2N(CH_2)_5$], 69.5, 68.5 [2 × s, CH of $C_5H_4CH_2CH_2N(CH_2)_5$], 61.5 [s, $CH_2CH_2N(CH_2)_5$], 55.3 [s, $(CH_2)_2N(CH_2)_2(CH_2)_2(CH_2)$], 28.1 [s, $CH_2CH_2N(CH_2)_5$], 26.9 [s, $(CH_2)_2N(CH_2)_2(CH_2)_2(CH_2)$], 25.3 [s, $(CH_2)_2N(CH_2)_2(CH_2)_2(CH_2)$].

**Fe{$\eta$-$C_5H_4CH_2(C_5H_4N)$}$_2$ (5)**. To a Schlenk tube charged with $FeCl_2$ (0.35 g, 0.003 mol) and THF (50 mL) was added a suspension of $NaC_5H_4CH_2(C_5H_4N)$ (1.0 g, 0.006 mol) in THF (30 mL) via cannula. The reaction mixture was stirred overnight. The solution was decanted, and the solvent was removed in vacuo. The product was washed with petroleum ether (bp 40−60 °C) and extracted with toluene (30 mL). Toluene was removed in vacuo to give a red-orange oil. Recrystallization from petroleum ether (bp 40−60 °C) afforded yellow crystalline needles (0.6 g, 0.0017 mol, 48%). $^1H$ NMR ($C_6D_6$, 250.1 MHz, 300 K): $\delta$ 8.43 [d, H, $C_5H_4CH_2C_5H_4N$], 7.48 [t, H, $C_5H_4CH_2C_5H_4N$], 7.26 [d, H, $C_5H_4CH_2C_5H_4N$], 7.04 [d of t, H, $C_5H_4CH_2C_5H_4N$], 4.03, 4.00 [2 × s, 4H, $C_5H_4CH_2C_5H_4N$], 3.78 [s, 2H, $C_5H_4CH_2C_5H_4N$]. $^{13}C\{^1H\}$ NMR ($C_6D_6$, 62.9 MHz, 300 K): $\delta$ 161.6 [s, $C_5H_4CH_2CC_4H_4N$], 149.4, 136.8, 122.8, 121.5 [4 × s, CH of $C_5H_4CH_2C_5H_4N$], 86.6 [s, $CCH_2$-

(14) Jutzi, P.; Redeker, T. *Eur. J. Inorg. Chem.* **1998**, 663−674.

$CC_4H_4N$], 69.8, 69.0 [2 × s, CH of $C_5H_4CH_2C_5H_4N$], 39.0 [s, $CH_2$ of $C_5H_4CH_2C_5H_4N$]

**[Fe{$\eta$-$C_5H_4(CH_2)_2NMe_3$}$_2$]$^{2+}$·2[I$^-$] (6)**. **1** (0.5 g, 0.0017 mol) was reacted with 2 equiv of methyl iodide (0.211 mL, 0.0034 mol) in diethyl ether, resulting in the formation of a yellow precipitate. The solid was washed with diethyl ether (3 × 15 mL) and any residual solvent removed under reduced pressure. The product was isolated as a light yellow powder (0.63 g, 65%). Anal. Calcd for $FeC_{18}H_{28}N_2I_2$: C, 39.2; H, 5.6; N, 4.6. Found: C, 38.7; H, 5.9; N, 4.3. $^1$H NMR ($CD_3OD$, 500.1 MHz, 300 K): $\delta$ 4.33, 4.23 [2 × virt t, 8H, $C_5H_4CH_2CH_2NMe_3$], 3.55 [m, 4H, $CH_2CH_2NMe_3$], 3.25 [s, 9H, $CH_2CH_2NMe_3$], 2.99 [m, 4H, $CH_2CH_2NMe_3$]. $^{13}$C{$^1$H} NMR ($CD_3OD$, 150 MHz, 300 K): $\delta$ 90.9 [s, $C(CH_2)_2NMe_3$], 70.9, 70.5 [2 × s, CH of $C_5H_4(CH_2)_2NMe_3$], 68.6 [s, $CH_2NMe_3$)], 54.3 [s, $C_5H_4(CH_2)_2NMe_3$], 25.0 [s, $CH_2CH_2NMe_3$]

**[Fe{$\eta$-$C_5H_4CH(CH_2)_4NMe_2$}$_2$]$^{2+}$·2[I$^-$] (7)**. **3** (0.3 g, 0.0008 mol) was reacted with 2 equiv of methyl iodide (0.100 mL, 0.0016 mol) in diethyl ether, resulting in the formation of a yellow precipitate. The solid was washed with diethyl ether (3 × 15 mL) and any residual solvent removed under reduced pressure. The product was isolated as a light yellow powder (0.41 g, 83%). Anal. Calcd for $FeC_{24}H_{38}N_2I_2$: C, 43.4; H, 5.8; N, 3.9. Found: C, 43.4; H, 5.8; N, 4.2. $^1$H NMR ($CD_3OD$, 500.1 MHz, 300 K): $\delta$ 4.11, 4.06 [2 × t, 8H, $C_5H_4CH(CH_2CH_2)_2NMe_2$], 3.50−3.42 [m, 4H, $CH(CH_2CH_2)_2NMe_2$], 3.13, 3.04 [2 × s, 6H, $CH(CH_2CH_2)_2NMe_2$] , 2.68 [tt, $^3J(^1H_{ax}-^1H_{ax})$ = 12.0 Hz, $^3J(^1H_{ax}-^1H_{eq})$ = 4.1 Hz, 2H, $CH(CH_2CH_2)_2NMe_2$], 2.03, 1.90−1.85 [2 × m, 8H, $CH(CH_2CH_2)_2NMe_2$]. $^{13}$C{$^1$H} NMR ($CD_3OD$, 150 MHz, 300 K): $\delta$ 93.2 [s, $CCH(CH_2CH_2)_2NMe_2$], 69.7, 68.3 [2 × s, CH of $C_5H_4CH(CH_2CH_2)_2NMe_2$], 64.2 [s, $CH(CH_2CH_2)_2NMe_2$], 57.2, 48.5 [s, $CH(CH_2CH_2)_2NMe_2$], 34.6 [s, CH of $CH(CH_2CH_2)_2NMe_2$], 29.5 [s, $CH_2$ of $(CH_2CH_2)_2NMe_2$].

**[Fe{$\eta$-$C_5H_4CH(CH_2)_4NHMe$}$_2$]$^{2+}$·2[$CF_3COO^-$] (8)**. **3** (0.158 g, 0.0008 mol) was reacted with an excess of trifluoroacetic acid in diethyl ether, resulting in the formation of an orange precipitate. The solid was washed with diethyl ether (3 × 15 mL) to remove any residual trifluoroacetic acid. The product was isolated as a light yellow powder and recrystallized as an orange solid from dichloromethane (0.15 g, 60%). Anal. Calcd for $FeC_{26}H_{34}N_2F_6O_4$: C, 51.3; H, 5.6; N, 4.6. Found: C, 51.4; H, 5.4; N, 4.6. $^1$H NMR ($CDCl_3$, 500.1 MHz, 300 K): $\delta$ 4.05, 3.98 [2 × s, 8H, $C_5H_4CH(CH_2CH_2)_2NHMe$], 3.58 [br s, 3H, $CH(CH_2CH_2)_2NHMe$], 2.74 [br s, 8H, $CH(CH_2CH_2)_2NHMe$], 2.26 [br s, 2H, $CH(CH_2CH_2)_2NHMe$], 2.02, [br s, 8H, $CH(CH_2CH_2)_2NHMe$]. $^{13}$C{$^1$H} NMR ($CDCl_3$, 150 MHz, 300 K): $\delta$ 163.0 [q, $CF_3COO^-$], 114.7 [s, $CF_3COO^-$], 91.8 [s, $CCH(CH_2CH_2)_2NHMe$], 68.1, 66.3 [2 × s, CH of $C_5H_4CH(CH_2CH_2)_2NHMe$], 54.5 [s, $CH(CH_2CH_2)_2NHMe$], 43.7 [s, $CH(CH_2CH_2)_2NHMe$], 31.9 [s, CH of $CH(CH_2CH_2)_2NHMe$], 29.6 [s, $CH_2$ of $(CH_2CH_2)_2NHMe$].

**[Fe{$\eta$-$C_5H_4CH(CH_2)_4NHMe$}$_2$]$^{2+}$·2[$BF_4^-$] (9)**. **3** (0.37 g, 0.001 mol) was reacted with an excess of $HBF_4$·OEt (54% in diethyl ether) in diethyl ether (100 mL). A yellow precipitate was immediately formed. The mixture was allowed to stir (10 min) and stand (10 min). The product was removed by filtration and washed with diethyl ether (3 × 15 mL) to give a yellow powder (0.32 g, 0.0006 mol, 63.9%). Anal. Calcd for $FeC_{22}H_{34}N_2B_2F_8$: C, 47.5; H, 6.2; N, 5.0. Found: C, 48.2; H, 6.3; N, 4.6. $^1$H NMR ($CD_3COCD_3$, 300 MHz, 300 K): $\delta$ 4.06, 4.02 [2 × virt t, 8H, $C_5H_4CH(CH_2CH_2)_2NHMe$], 3.49 [br m, 4H, eq $CH(CH_2CH_2)_2NHMe$], 2.99 [td, 4H, ax $CH(CH_2CH_2)_2NHMe$], 2.80 [s, 6H, $CH(CH_2CH_2)_2NHMe$], 2.51 [tt, $^3J(^1H_{ax}-^1H_{ax})$ = 12.0 Hz, $^3J(^1H_{ax}-^1H_{eq})$ = 3.9 Hz, 2H, $CH(CH_2CH_2)_2NHMe$], 2.09, [br m, 4H, eq $CH(CH_2CH_2)_2NHMe$], 1.87 [br m, 4H, ax $CH(CH_2CH_2)_2NHMe$]. $^{13}$C{$^1$H} NMR ($CD_3COCD_3$, 300 MHz, 300 K): $\delta$ 92.5 [s, $CCH(CH_2CH_2)_2NHMe$], 67.8, 66.4 [2 × s, CH of $C_5H_4CH(CH_2CH_2)_2NHMe$], 54.9 [s, $CH(CH_2CH_2)_2NHMe$], 43.6 [s, $CH(CH_2CH_2)_2NHMe$], 32.7 [s, CH of $CH(CH_2CH_2)_2NHMe$], 30.8 [s, $CH_2$ of $(CH_2CH_2)_2NHMe$].

**[Fe{$\eta$-$C_5H_4(CH_2)_2NCH_3(CH_2)_5$}$_2$]$^{2+}$·2[I$^-$] (10)**. **4** (0.2 g, 0.0005 mol) was reacted with 2 equiv of methyl iodide (0.06 mL, 0.001 mol) in diethyl ether, resulting in the formation of a yellow precipitate. The solid was washed with diethyl ether (3 × 15 mL) and any residual solvent removed under reduced pressure. The product was isolated as a light yellow powder (0.29 g, 88%). Anal. Calcd for $FeC_{26}H_{42}N_2I_2$ C 45.1; H 6.1; N 4.0. Found: C, 46.0; H, 6.3; N, 3.9. $^1$H NMR ($CD_3OD$, 500.1 MHz, 300 K): 4.34, 4.23 [2 × virt t, 8H, $C_5H_4(CH_2)_2NMe(CH_2)_5$], 3.44−3.36 [m, 8H, $CH_2CH_2NMe(CH_2)_2(CH_2)_2(CH_2)$], 3.10 [m, 6H, $(CH_2)_2NMe(CH_2)_2(CH_2)_2(CH_2)$], 2.90 [m, 4H, $CH_2CH_2NMe(CH_2)_5$], 1.86 [m, 8H, $(CH_2)_2NMe(CH_2)_2(CH_2)_2(CH_2)$], 1.66 [m, 4H, $(CH_2)_2NMe(CH_2)_2(CH_2)_2(CH_2)$]. $^{13}$C{$^1$H} NMR ($CD_3OD$, 150 MHz, 300 K): $\delta$ 83.5 [s, $C(CH_2)_2NMe(CH_2)_5$], 69.6, 69.1 [2 × s, CH of $C_5H_4CH_2CH_2NMe(CH_2)_5$], 65.1, 61.4 [2 × s, $CH_2CH_2NMe(CH_2)_5$ and $(CH_2)_2NMe(CH_2)_2(CH_2)_2(CH_2)$], 47.1 [s, $CH_2CH_2NMe(CH_2)_5$], 22.5 [s, $CH_2CH_2NMe(CH_2)_5$], 21.0 [s, $(CH_2)_2NMe(CH_2)_2(CH_2)_2(CH_2)$], 20.1 [s, $(CH_2)_2NMe(CH_2)_2(CH_2)_2(CH_2)$].

**[Fe{$\eta$-$C_5H_4(CH_2)_2NH(CH_2)_5$}$_2$]$^{2+}$·2[$CF_3CO_2^-$] (11)**. **4** (1.02 g, 0.0025 mol) was reacted with an excess of trifluoroacetic acid in diethyl ether (100 mL). A yellow precipitate was formed after stirring (5 min). The solid was washed with diethyl ether (3 × 15 mL). The product was isolated as a yellow powder (1.1 g, 0.0018 mol, 71%). Crystals of the product were obtained from a toluene−diethyl ether mixture. Anal. Calcd for $FeC_{28}H_{38}N_2O_4F_6$: C, 52.8; H, 6.0; N, 4.4. Found: C, 52.6; H, 6.1; N, 4.3. $^1$H NMR ($CDCl_3$, 300 MHz, 300 K): $\delta$ 4.00, 3.96 [2 × br s, 8H, $C_5H_4(CH_2)_2N(CH_2)_5$], 3.6 [d, 4H, ax or eq $(CH_2)_2N(CH_2)_2(CH_2)_2(CH_2)$], 2.56 [br s, 4H, ax or eq $(CH_2)_2N(CH_2)_2(CH_2)_2(CH_2)$], 2.96 [br s, 4H, $C_5H_4CH_2CH_2N(CH_2)_5$], 2.76 [br s, 4H, $(C_5H_4CH_2CH_2N(CH_2)_5$], 1.94 [br m, 2H, ax or eq $N(CH_2)_2(CH_2)_2(CH_2)$], 1.35 [br m, 2H, ax or eq $N(CH_2)_2(CH_2)_2(CH_2)$], 1.90 [br m, 4H, $N(CH_2)_2(CH_2)_2(CH_2)$]. $^{13}$C{$^1$H} NMR ($CDCl_3$, 300 MHz, 300 K): $\delta$ 83.3 [s, $C(CH_2)_2N(CH_2)_5$], 69.1, 68.5 [2 × s, CH of $C_5H_4CH_2CH_2N(CH_2)_5$], 58.1 [s, $CH_2CH_2N(CH_2)_5$], 53.4 [s, $(CH_2)_2N(CH_2)_2(CH_2)_2(CH_2)$], 24.0 [s, $CH_2CH_2N(CH_2)_5$], 22.9 [s, $(CH_2)_2N(CH_2)_2(CH_2)_2(CH_2)$], 22.1 [s, $(CH_2)_2N(CH_2)_2(CH_2)_2(CH_2)$].

**[Fe{$\eta$-$C_5H_4(CH_2)_2NH(CH_2)_5$}$_2$]$^{2+}$·2[$BF_4^-$] (12)**. **4** (1 g, 0.0025 mol) was reacted with an excess of $HBF_4$·OEt (54% in diethyl ether) in diethyl ether (100 mL). A yellow precipitate was immediately formed. The mixture was allowed to stir (10 min) and stand (10 min). The product was removed by filtration and washed with diethyl ether (3 × 15 mL) to give a yellow powder (0.81 g, 0.0014 mol, 56%). Crystals of the product were obtained via vapor diffusion from acetone and diethyl ether. Anal. Calcd for $FeC_{24}H_{38}N_2B_2F_8$: C, 49.4; H, 6.6; N, 4.9. Found: C, 51.1; H, 7.1; N, 5.2. $^1$H NMR ($CD_3COCD_3$, 300 MHz, 300 K): $\delta$ 4.15, 4.09 [2 × s, 8H, $(C_5H_4(CH_2)_2N]$, 3.29 [s, 12H, $CH_2CH_2N(CH_2)_2(CH_2)_2(CH_2)$], 2.82 [s, 4H, $(C_5H_4CH_2CH_2N(CH_2)_5]$, 1.84 [s, 8H, $N(CH_2)_2(CH_2)_2(CH_2)$], 1.53 [s, 4H, $N(CH_2)_2(CH_2)_2(CH_2)$. $^{13}$C{$^1$H} NMR ($CD_3COCD_3$, 300 MHz, 300 K): $\delta$ 84.6 [s, $C(CH_2)_2N(CH_2)_5$], 69.1, 68.8 [2 × s, CH of $C_5H_4CH_2CH_2N(CH_2)_5$], 58.2 [s, $CH_2CH_2N(CH_2)_5$], 53.5 [s, $(CH_2)_2N(CH_2)_2(CH_2)_2(CH_2)$], 24.3 [s, $CH_2CH_2N(CH_2)_5$], 23.7 [s, $(CH_2)_2N(CH_2)_2(CH_2)_2(CH_2)$], 22.2 [s, $(CH_2)_2N(CH_2)_2(CH_2)_2(CH_2)$].

**[Fe{$\eta$-$C_5H_4CH(CH_2)_4NHMe$}$_2$]$^{3+}$·3[$BF_4^-$] (13)**. To a Schlenk tube charged with *p*-benzoquinone (0.016 g, 0.00015 mol), $HBF_4$·OEt (54% in diethyl ether, 0.081 mL, 0.00059 mol), and diethyl ether (50 mL) was added **4** (0.18 g, 0.0003 mol) in diethyl ether (50 mL) via cannula. A blue solid was immediately precipitated.

The mixture was allowed to stir (10 min) and stand (10 min). The blue solid was removed by filtration and washed with diethyl ether (30 mL).

Recrystallization via vapor diffusion from deoxygenated acetone and diethyl ether afforded blue crystals (0.14 g, 0.0002 mol, 72%). Found: C, 41.7; H, 5.4; N, 4.6. Anal. Calcd for $FeC_{20}H_{34}N_2B_3F_{12}$: C, 41.1; H, 5.3; N, 4.4.

**$[Fe\{\eta\text{-}C_5H_4CH(CH_2)_4NMe_2\}_2]^{3+}\cdot 3[BF_4^-]$ (14)**. To a Schlenk tube charged with *p*-benzoquinone (0.0073 g, 0.00007 mol), $HBF_4\cdot OEt_2$ (54% in diethyl ether, 0.037 mL, 0.0003 mol), and diethyl ether (50 mL) was added **7** (0.09 g, 0.0001 mol) in diethyl ether (50 mL) via cannula. A blue solid was immediately precipitated. The mixture was allowed to stir (20 min) and stand (10 min). The blue solid was removed by filtration and washed with diethyl ether (30 mL) (0.05 g, 0.00008 mol, 78%). The crude product was purified by dissolution in acetone (100 mL), filtration, and precipitation by addition of diethyl ether (150 mL) to give a blue powder (0.027 g, 0.00004 mol, 39%). Anal. Calcd for $FeC_{24}H_{38}N_2B_3F_{12}$: C, 43.0; H, 5.7; N, 4.2. Found: C, 43.1; H, 5.9; N, 4.1.

**$[Fe\{\eta\text{-}C_5H_4(CH_2)_2NH(CH_2)_5\}_2]^{3+}\cdot 3[BF_4^-]$ (15). Method 1**. To a Schlenk tube charged with *p*-benzoquinone (0.04 g, 0.00032 mol), $HBF_4\cdot OEt_2$ (54% in diethyl ether, 1 mL, 0.0072 mol), and diethyl ether (50 mL) was added **11** (0.1 g, 0.00016 mol) in diethyl ether (50 mL) via cannula. A blue solid was immediately precipitated. The mixture was allowed to stir (20 min) and stand (10 min). The blue solid was removed by filtration and washed with diethyl ether (30 mL).

The crude product was purified by dissolution in acetone (100 mL), filtration, and precipitation by addition of diethyl ether (150 mL) to give a blue powder (0.06 g, 0.000083 mol, 52%). Blue crystals suitable for X-ray analysis were obtained via vapor diffusion from acetone and diethyl ether.

**Method 2**. To a Schlenk tube charged with *p*-benzoquinone (0.135 g, 0.00125 mol), $HBF_4\cdot OEt_2$ (54% in diethyl ether, 1 mL, 0.0072 mol), and diethyl ether (50 mL) was added **4** (0.71 g, 0.00175 mol) in diethyl ether (50 mL) via cannula. A blue solid was immediately precipitated. The mixture was allowed to stir (20 min) and stand (10 min). The blue solid was removed by filtration and washed with diethyl ether (30 mL).

The crude product was purified by dissolution in acetone (100 mL), filtration, and precipitation by addition of diethyl ether (150 mL) to give a blue powder (0.93 g, 0.0015 mol, 83%). Blue crystals suitable for X-ray analysis were obtained via vapor diffusion from acetone and diethyl ether. Anal. Calcd for $FeC_{26}H_{42}N_2B_3F_{12}$: C, 42.8; H, 5.7; N, 4.2. Found: C, 42.5; H, 6.1 N, 4.2.

**Crystallographic Data Collection and Structure Analysis. X-ray Crystallography**. Data for compounds **4**, **5**, **8**, **11**−**13**, and **15** were collected on a Nonius Kappa CCD area detector diffractometer using graphite-monochromated Mo Kα radiation ($\lambda$ = 0.71073 Å) using 1.0 $\phi$ rotation frame. Pertinent crystallographic details are given in Table 1. The structures of all seven compounds were solved by direct methods using SHELXS 86. Refinement, by full-matrix least-squares methods on $F^2$ using SHELXL 97, was similar for all seven compounds. Non-hydrogen atoms were constrained to idealized positions using a riding model (with free rotation for methyl groups).

## Results and Discussion

**Ferrocene Compounds**. The synthetic methodology used to prepare the amino-functionalized ferrocene compounds is quite general. $Fe\{\eta\text{-}C_5H_4(CH_2)_2NMe_2\}_2$ (**1**), $Fe\{\eta\text{-}C_5H_4(CH_2)_3NMe_2\}_2$ (**2**), $Fe\{\eta\text{-}C_5H_4CH(CH_2)_4NMe\}_2$ (**3**), $Fe\{\eta\text{-}C_5H_4(CH_2)_2N(CH_2)_5\}_2$ (**4**), and $Fe\{\eta\text{-}C_5H_4CH_2(C_5H_4N)\}_2$ (**5**) are readily prepared by addition of 2 equiv of the corresponding sodium cyclopentadienide salts as a THF slurry to anhydrous $FeCl_2$ in THF (Scheme 1). Stirring the brown mixture overnight resulted in a change of color to orange with concomitant formation of a beige precipitate (NaCl). After removal of the solvent under reduced pressure, the product was extracted into toluene and dried in vacuo.

**Scheme 1**[a]

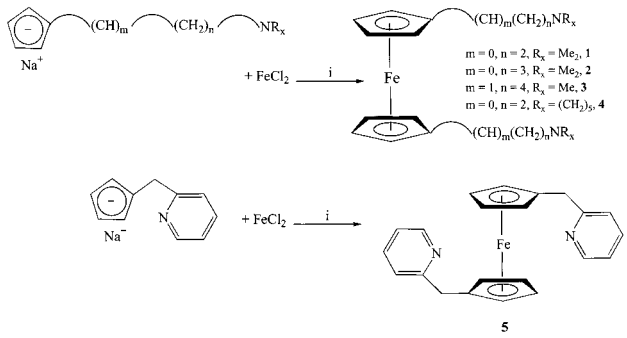


[a] Reagent: (i) THF.

Compounds **1**−**5** were characterized by microanalysis, NMR spectroscopy, mass spectrometry, and, in the case of **3**−**5**, X-ray crystallography. Repeated attempts at acquiring microanalytical data for **4** and **5** proved to be unsuccessful. Some characterization data of **1**[15] have been previously reported, but we have found that simple isolation of **1**, without high-vacuum techniques, yields analytically pure material. Changing the alkyl group between the cyclopentadienyl and the nitrogen atom has a dramatic effect on the physical properties of the compounds. For example, compounds **1** and **2** are oils, **3** is an oily crystalline solid, and **4** and **5** are crystalline solids. Therefore, by making the pendant arm more rigid, the crystalline nature of the resultant compound increases.

The $^1H$ and $^{13}C$ NMR spectra for **1**−**5** are as expected, with the shifts for the $CH_2$ groups next to the nitrogen atoms occurring at a higher $\delta$ (ppm) than those for the other $CH_2$ groups. $^1H$ NMR spectroscopy shows chemical shifts for the protons attached to the cyclopentadienyl moieties occurring at $\delta$ 3.92−4.02 ppm for compounds **1**−**5**. The chemical shifts for the methyl groups attached to the nitrogen atoms for compounds **1**−**3** are quite distinctive, occurring at $\delta$ 2.18−2.29 and 45.4−47.0 ppm for the $^1H$ and $^{13}C$ NMR spectra, respectively. Of particular interest is the NMR of **3**, which shows signals attributable to axial and equatorial protons of the piperidyl ring. $^1H-^1H$ and $^1H\{^{13}C\}$ NMR spectroscopy correlation experiments proved particularly useful in determining that the axial protons are furthest downfield in the $^1H$ NMR spectrum. Thus, for **3,** there is quite a large difference in chemical shift of the axial, $\delta$ 2.90 ppm, and equatorial, 1.97−1.15 ppm, protons which are attached to the carbon atoms next to the nitrogen. The differences in the chemical shifts associated with the axial and equatorial

(15) Rees, W. S., Jr.; Lay, U. W.; Dippel, K. A. *J. Organomet. Chem.* **1994**, *483*, 27−31.

**Scheme 2**[a]

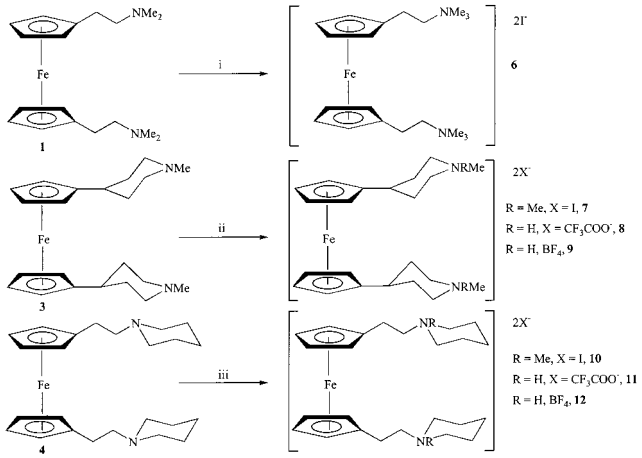


[a] Reagents: (i) MeI, (ii) MeI, $CF_3COOH$, or $HBF_4$, (iii) MeI, $CF_3COOH$, or $HBF_4$.

protons are the result of the trans diaxial relationship between the C−H and the nitrogen lone pair. The $^1$H NMR resonance for the $CH_2$ group for compound **5** occurs at $\delta$ 3.78 ppm, which is at least 1 ppm greater than the shifts for the $CH_2$ groups next to the nitrogen atoms; this could be due to the extra electron-withdrawing power of the pyridyl ring. The corresponding $^{13}$C NMR occurs at $\delta$ 39.0 ppm, which is also greater than expected for a $CH_2$ group next to the cyclopentadienyl ring.

**Ferrocene Salt Compounds**. Methylation of the pendant amino functionality of **1**, **3**, and **4** has been achieved by the addition of ether solutions of methyl iodide to yield the ferrocene salts **6**, **7**, and **10** in high yield, ∼80%, as shown in Scheme 2. Characterization of these compounds was achieved by microanalysis and NMR spectroscopy.

$^1$H NMR spectroscopy for compound **7** in $d_4$-methanol shows the expected additional resonance for the methyl group at 3.10 ppm (compared to **3**), and for compound **10** there are two signals for the methyl groups at 3.13 and 3.04 ppm; the corresponding shift for the three methyl groups for compound **6** occurs at 3.25 ppm. Although the NMR spectra are carried out in different solvents, the shifts are approximately 1 ppm further downfield than those of the corresponding neutral ferrocenes **1**, **3**, and **4**. This trend is expected when an amino group is quaternerized and is also evident for the methyl signals in the $^{13}$C spectra, where there is approximately a shift of 9−10 ppm for compounds **6** and **7**. A similar phenomenon was noticed for the $CH_2$ next to the amino functionality, where there was a shift downfield of approximately 0.8 ppm in the $^1$H NMR spectrum for **1**, **3**, and **4** and a corresponding shift of 4−7 ppm downfield for the $^{13}$C spectra. For a specific case, methylation of the nitrogen atom of **3** leads to the merging of the chemical shifts for the $CH_2$ axial and equatorial protons attached to the carbon atoms bound to the nitrogen atom. Other compounds, where the amino functionality is bound directly to the ring, have been reported previously.[16] For these compounds both monomethylation and dimethylation of the amino functional groups of 1,1′-bis(*N*,*N*-dimethylamino)ferrocene have been reported. Our reactions differ in that we obtain exclusively the dimethyl products when 1 or 2 equiv of methyl iodide is added to the ferrocenes.

**Scheme 3**[a]

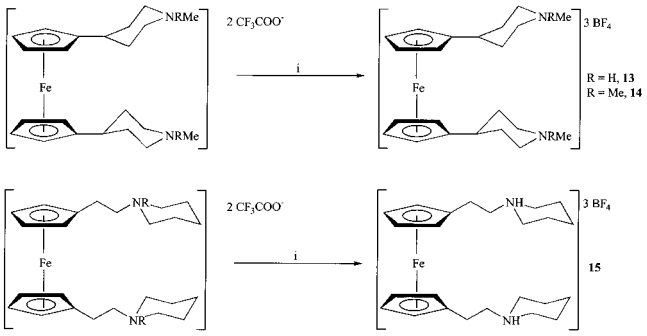


[a] Reagents: (i) ether/$HBF_4$/*p*-benzoquinone.

Protonation of **3** and **4** was achieved by addition of $CF_3COOH$ to an ether solution of **3** and **4** to yield light orange powders of $[Fe\{\eta\text{-}C_5H_4CH(CH_2)_4NHMe\}_2]^{2+}\cdot 2[CF_3CO_2^-]$ (**8**) and $[Fe\{\eta\text{-}C_5H_4(CH_2)_2NH(CH_2)_5\}_2]^{2+}\cdot 2[CF_3CO_2^-]$ (**11**), as shown in Scheme 2. Addition of $HBF_4$ to **3** and **4** afforded the analogous ionic compounds **9** and **12** with $BF_4$ as the counterion (Scheme 2). Recrystallization of **8** and **11** from $CH_2Cl_2$ yielded X-ray-quality orange crystals, whereas **12** was recrystallized from acetone/ether; further characterization was achieved by microanalysis and NMR spectroscopy. Thus, **8**, **9**, **11**, and **12** proved to be much more soluble than the methylated ferrocenes **6**, **7**, and **10**, which only proved to be soluble in protic solvents such as methanol, ethanol, and water.

**Ferrocenium Salt Compounds**. Oxidation of the ferrocene salts **7**, **8**, and **11** results in the formation of the ferrocenium species **13**−**15**, as shown in Scheme 3. This was achieved by the addition of a *p*-benzoquinone and an ether solution of $HBF_4$, following the method of Connelly et al.[17] An interesting point to note is that during the oxidation process the trifluoroacetate anions are replaced by tetrafluoroborate anions: oxidation of one of the neutral ferrocenes, **4**, also produces **15**. A blue solid was obtained in each case, and characterization of these paramagnetic compounds was achieved using microanalysis and X-ray crystallography in the case of **13** and **15**.

**Crystallography**. The pertinent crystallographic details for **4**, **5**, **8**, **11**−**13**, and **15** are given in Table 1.

**Ferrocene Compounds**. The crystal structure of **3** was published in a previous paper.[6] There are some notable comparisons to be made to the structures obtained in this paper. Crystals of **4** were obtained by slow evaporation from an ether solution, and an X-ray structure analysis was carried out. Selected bond lengths and angles are shown in Table 2. Compound **4** is the first structurally characterized example of a metal complex containing the $C_5H_4(CH_2)_2N(CH_2)_5$ ligand and the molecular structure is shown in Figure 1.

(16) Stahl, K.-P.; Boche, G.; Massa, W. *J. Organomet. Chem.* **1984**, *486*, 291.
(17) Connelly, N. G.; Geiger, W. E. *Chem. Rev.* **1996**, *96*, 877−910.

**Table 1.** Crystallographic Data for Compounds **4**, **5**, **8**, **11**−**13**, and **15**

| | **4** | **5** | **8** | **11** | **12** | **13** | **15** |
|---|---|---|---|---|---|---|---|
| empirical formula | $C_{24}H_{36}FeN_2$ | $C_{22}H_{20}FeN_2$ | $C_{26}H_{34}F_6FeN_2O_4$ | $C_{28}H_{38}F_6FeN_2O_4$ | $C_{24}H_{38}B_2F_8FeN_2$ | $C_{22}H_{34}B_3F_{12}FeN_2$ | $C_{24}H_{38}B_3F_{12}FeN_2$ |
| fw | 408.4 | 368.25 | 608.4 | 636.45 | 584.03 | 642.79 | 670.84 |
| cryst syst | monoclinic | triclinic | triclinic | monoclinic | monoclinic | monoclinic | triclinic |
| space group | $P2_1/c$ | $P\bar{1}$ | $P\bar{1}$ | $P2_1$ | $P2_1/c$ | $C2/c$ | $P\bar{1}$ |
| *a*, Å | 6.0088(2) | 5.8396(3) | 11.53790(10) | 7.39400(10) | 13.4954(2) | 26.5138(7) | 12.40280(10) |
| *b*, Å | 11.1680(4) | 16.1100(8) | 12.9269(2) | 12.2973(2) | 6.16440(10) | 7.9306(3) | 14.1872(2) |
| *c*, Å | 15.7744(5) | 19.9913(10) | 13.8330(2) | 16.4000(3) | 31.6684(6) | 15.3975(5) | 18.6994(2) |
| α, deg | 90 | 114.054(2) | 96.2130(8) | | | | 93.8530(5) |
| *β*, deg | 96.506(3) | 95.030(3) | 90.7990(8) | 102.7110(3) | 94.4780(6) | 123.6610(10) | 99.2720(6) |
| *γ*, deg | 90 | 95.368(3) | 96.0790(5) | | | | 113.7380(6) |
| vol, Å$^3$ | 1051.74(6) | 1693.40(12) | 2038.86(5) | 1454.64(4) | 2626.48(8) | 2694.79(15) | 2940.70(6) |
| temp, K | 150(2) | 150(2) | 150(2) | 150(2) | 150(2) | 150(2) | 150(2) |
| Z | 2 | 4 | 3 | 2 | 4 | 4 | 4 |
| $\mu$(Mo Kα), mm$^{-1}$ | 0.728 | 0.896 | 0.631 | 0.593 | 0.648 | multiscan | multiscan |
| no. of reflns collected | 14428 | 6584 | 37964 | 26747 | 21359 | 9435 | 57220 |
| no. of independent reflns | 2071 | 5414 | 7970 | 5668 | 5167 | 4836 | 11530 |
| $R_{int}$[a] | 0.064 | 0.0468 | 0.0529 | 0.0589 | 0.0685 | 0.0412 | 0.0799 |
| final *R* indices [$I > 2\sigma(I)$], R1[b] | 0.0335 | 0.0396 | 0.0368 | 0.0416 | 0.0491 | 0.0449 | 0.0637 |
| wR2[c] | 0.0858 | 0.0903 | 0.0943 | 0.1016 | 0.1103 | 0.1337 | 0.1764 |

[a] $R_{int} = \sum|F_o^2 - F_o^2(\text{mean})|/\sum[F_o^2]$. [b] $R1 = \sum||F_o| - |F_c||/\sum|F_o|$. [c] $wR2 = [\sum[w(F_o^2 - F_c^2)^2]/\sum[w(F_o^2)^2]]^{1/2}$.

**Table 2.** Selected Interatomic Distances (Å) and Selected Angles (deg) between Interatomic Vectors with Estimated Standard Deviations in Parentheses for **4**[a]

| | | | |
|---|---|---|---|
| Fe(1)−C(1) | 2.0516(17) | C(1)−C(2) | 1.420(2) |
| Fe(1)−C(2) | 2.0402(17) | C(2)−C(3) | 1.422(3) |
| Fe(1)−C(3) | 2.0382(17) | C(3)−C(4) | 1.407(3) |
| Fe(1)−C(4) | 2.0515(19) | C(4)−C(5) | 1.420(3) |
| Fe(1)−C(5) | 2.0480(18) | C(5)−C(1) | 1.419(2) |
| average Fe−C | 2.05 | average C−C | 1.42 |
| C(1)−C(2)−C(3) | 108.33(17) | average C−C−C | 108 |
| C(2)−C(3)−C(4) | 108.16(16) | C(6)−C(1)−Cp(cent)(1) | 178.8 |
| C(3)−C(4)−C(5) | 107.72(17) | | |
| C(4)−C(5)−C(1) | 108.77(16) | | |
| C(5)−C(1)−C(2) | 107.01(16) | | |
| Fe(1)−Cp(cent)(1) | 1.66 | | |

[a] Cp(cent)(1) denotes the centroid of the $C_5$ rings C(1)−C(5) and C(1)′∠C(5)′.

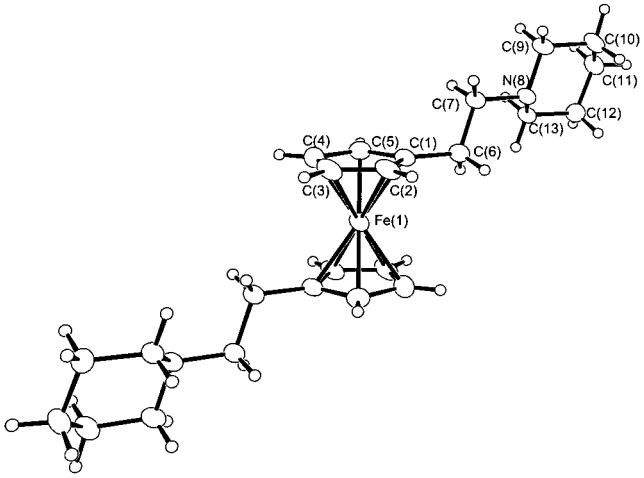


**Figure 1.** Molecular structure of compound **4**.

Other metal complexes featuring the $C_5H_4(CH_2)_2N(CH_2)_5$ ligand system include Ti{$\eta$-$C_5H_4(CH_2)_2N(CH_2)_5$}$Cl_3$[18] and Cr{$\eta$-$C_5H_4(CH_2)_2N(CH_2)_5$}$Cl_2$.[19] The compound Ti{$\eta$-$C_5H_4$-$(CH_2)_2N(CH_2)_5$}$Cl_3$ was synthesized by treatment of $TiCl_4$ with $Me_3SiC_5H_4(CH_2)_2N(CH_2)_5$, but no characterization data have been published. The chromium analogue Cr{$\eta$-$C_5H_4$-$(CH_2)_2N(CH_2)_5$}$Cl_2$ was characterized by elemental analysis and mass spectrometry. **4** has half of a molecule per asymmetric unit and a crystallographic center of inversion; this compares to **3**, which has one molecule per asymmetric unit. The piperidin-*N*-ylethyl ring substituents exist in a chair conformation, which is similar to the conformation of the methyl-substituted piperidinyl ring in **3**. Compound **4** differs from **3** in that the cyclopentadienyl rings are staggered from each other and the piperidin-*N*-ylethyl side chains are as far away from each other as possible. For **3**, the cyclopentadienyl rings are virtually eclipsed and the substituents are not completely opposite each other. We have observed a similar phenomenon for the analogous vanadocene systems.[20]

The (pyrid-2-ylmethyl)cyclopentadienyl ligand system has been used previously in the synthesis of titanocene derivatives; the hydrolysis product $([Ti\{\eta\text{-}C_5H_4CH_2(C_5H_4NH)\}Cl_2]_2O)^{2+}\cdot 2[Cl^-]$ was obtained during the attempted preparation of Ti{$\eta$-$C_5H_4CH_2(C_5H_4N)$}$Cl_3$.[21] This is the first time that this ligand has been crystallographically characterized while attached to a metal center. Single crystals of **5** were obtained from slow evaporation from a solution in toluene. The two cyclopentadienyl rings of the ferrocene unit are eclipsed, with the pyrid-2-ylmethyl side chains trans to each other, which is similar to the conformation adopted in **3**. But, unlike **3** and **4**, there are two molecules of **5** per asymmetric unit. Selected data for molecule 1 and molecule 2 are given in Table 3.

The iron ring−centroid distances for molecule 1 are Fe(1)−Cp(cent) = 1.640 Å and Fe(1)−Cp(cent) = 1.636 Å, and those for molecule 2 are Fe(2)−Cp(cent) = 1.650 Å and Fe(2)−Cp(cent) = 1.651 Å; these are not exceptional for these types of cyclopentadienyl systems, but it should

(18) Herrmann, W. A.; Morawietz, M. J. A.; Priermeier, T.; Mashima, K. *J. Organomet. Chem.* **1995**, *486*, 291−295.
(19) Döhring, A.; Göhre, J.; Jolly, P. W.; Kryger, B.; Rust, J.; Verhovnik, G. P. J. *Organometallics* **2000**, *19*, 388−402.
(20) Bradley, S.; McGowan, P. C. Unpublished work.
(21) Blais, M. S.; Chien, J. C. W.; Rausch, M. D. *Organometallics* **1998**, *17*, 3775−3783.

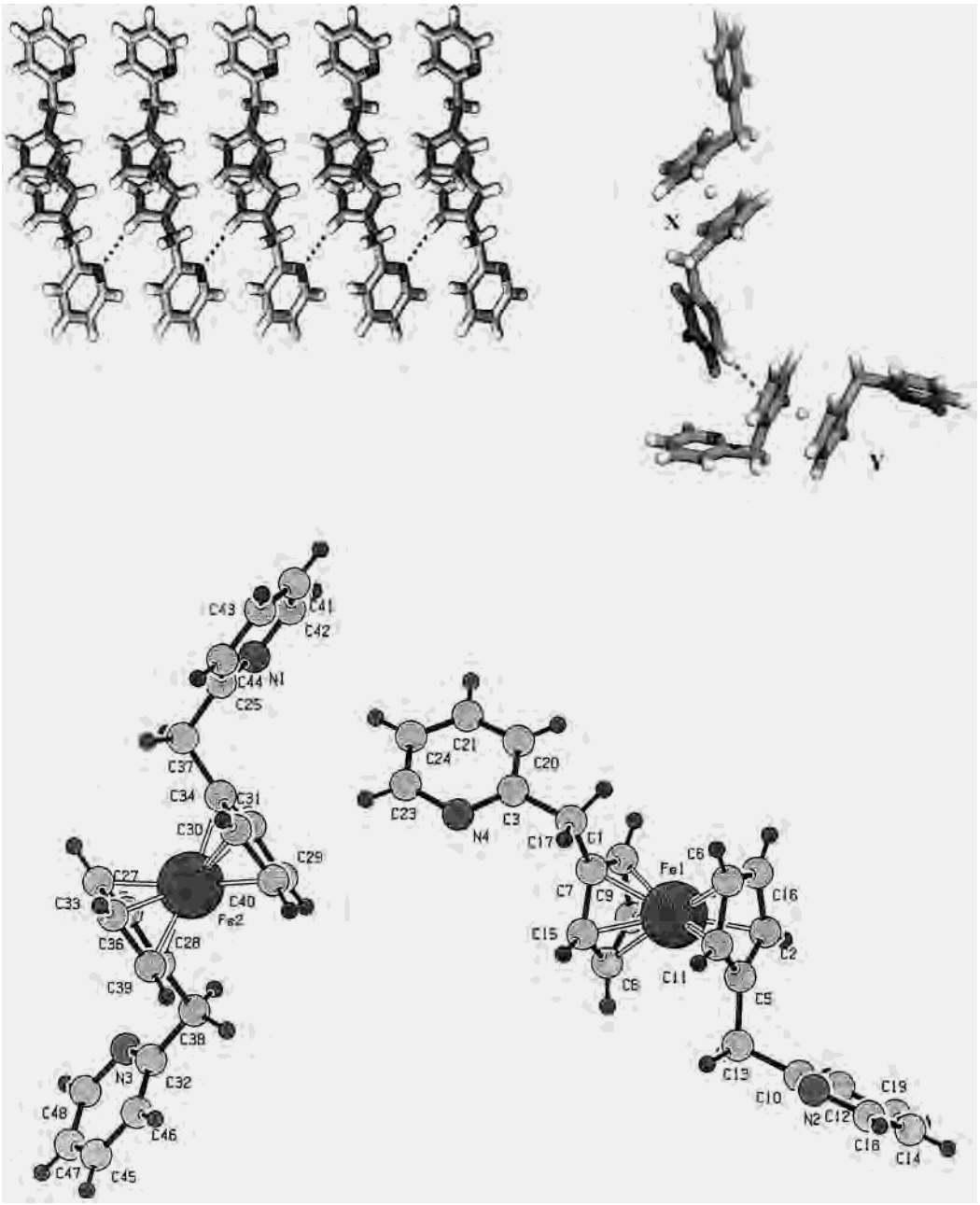


**Figure 2.** (a, top left) Chains of molecule 1 of compound **5** which are linked by C−H···N interactions. The C−H···N distance and angle are 2.37 Å and 166°. (b, top right) One of the C−H···$\pi$-linked chains of molecule 2 with molecule 1. The C−H···$\pi$ distance and angle are 2.617 Å and 153°. (c, bottom) The asymmetric unit of compound **5** containing two molecules (molecule 1 and molecule 2).

be noted that they are different from each other. The distances for molecule 2 are also slightly shorter than those of **3** and **4** (1.657/1.660 and 1.660 Å, respectively), especially in the case of molecule 1. Compared to the crystal structures of **3** and **4**, the packing of **5** is dramatically different.

To evaluate whether there were any short intermolecular distances in **5**, the crystallographic data were subjected to a Platon analysis:[22] Platon is a molecular geometry tool, which provides bond lengths and angles for intermolecular separations which are shorter than expected. The Platon analysis showed that there is a short contact between one of the *ortho* C−H groups of a cyclopentadienyl unit and the nitrogen of the pyridyl moiety of an adjacent molecule 1, giving a distance C−H···N of 2.57 Å and a C−H−N angle of 166°. This is significantly shorter than the sum of the van der Waals radii of 2.75 Å. Thus, these interactions lead to intermolecular bonds which result in chains of molecule 1 linked by the C−H···N interactions within the crystal lattice. This is highlighted in Figure 2a.

There are no such intermolecular interactions involved in molecule 2, but molecule 2 experiences a weak C−H···$\pi$ cloud interaction with the hydrogen atom next to the nitrogen atom of its pyridyl ring, C(23)−H(23), and one of the Cp centroids of molecule 1; this is shown in Figure 2b. The

(22) Spek, A. L. *PLATON A Multipurpose Crystallographic Tool*; Utrecht University: Utrecht, The Netherlands, 2000.

**Table 3.** Selected Interatomic Distances (Å) and Selected Angles (deg) between Interatomic Vectors with Estimated Standard Deviations in Parentheses for **5**[a]

| molecule 1 | | molecule 2 | |
|---|---|---|---|
| Fe(1)−C(1) | 2.020(2) | Fe(2)−C(23) | 2.054(2) |
| Fe(1)−C(2) | 2.043(2) | Fe(2)−C(24) | 2.027(2) |
| Fe(1)−C(3) | 2.040(2) | Fe(2)−C(25) | 2.037(3) |
| Fe(1)−C(4) | 2.043(3) | Fe(2)−C(26) | 2.039(2) |
| Fe(1)−C(5) | 2.006(2) | Fe(2)−C(27) | 2.023(2) |
| Fe(1)−C(12) | 2.035(2) | Fe(2)−C(34) | 2.028(2) |
| Fe(1)−C(13) | 2.042(2) | Fe(2)−C(35) | 2.040(2) |
| Fe(1)−C(14) | 2.047(3) | Fe(2)−C(36) | 2.028(2) |
| Fe(1)−C(15) | 2.017(2) | Fe(2)−C(37) | 2.049(3) |
| Fe(1)−C(16) | 1.988(2) | Fe(2)−C(38) | 2.028(2) |
| C(1)−C(2) | 1.389(3) | C(23)−C(24) | 1.390(4) |
| C(2)−C(3) | 1.414(4) | C(24)−C(25) | 1.421(4) |
| C(3)−C(4) | 1.396(4) | C(25)−C(26) | 1.383(3) |
| C(4)−C(5) | 1.406(3) | C(26)−C(27) | 1.415(3) |
| C(5)−C(1) | 1.428(3) | C(27)−C(23) | 1.403(3) |
| C(12)−C(13) | 1.393(3) | C(34)−C(35) | 1.378(3) |
| C(13)−C(14) | 1.423(4) | C(35)−C(36) | 1.403(4) |
| C(14)−C(15) | 1.389(3) | C(36)−C(37) | 1.396(3) |
| C(15)−C(16) | 1.413(3) | C(37)−C(38) | 1.392(4) |
| C(16)−C(12) | 1.403(3) | C(38)−C(34) | 1.418(3) |
| average Fe−C | 2.04 | average Fe−C | 2.04 |
| average C−C | 1.407 | average C−C | 1.4 |
| Fe(1)−Cp(cent)(1) | 1.64 | Fe(2)−Cp(cent)(3) | 1.65 |
| Fe(1)−Cp(cent)(2) | 1.636 | Fe(2)−Cp(cent)(4) | 1.65 |
| C(1)−C(2)−C(3) | 107.5(2) | C(23)−C(24)−C(25) | 109.6(2) |
| C(2)−C(3)−C(4) | 109.5(5) | C(24)−C(25)−C(26) | 107.3(2) |
| C(3)−C(4)−C(5) | 106.9(2) | C(25)−C(26)−C(27) | 107.5(2) |
| C(4)−C(5)−C(1) | 108.3(2) | C(26)−C(27)−C(23) | 109.4(2) |
| C(5)−C(1)−C(2) | 107.8(2) | C(27)−C(23)−C(24) | 106.1(2) |
| C(12)−C(13)−C(14) | 109.0(2) | C(34)−C(35)−C(36) | 107.4(2) |
| C(13)−C(14)−C(15) | 107.4(2) | C(35)−C(36)−C(37) | 109.6(2) |
| C(14)−C(15)−C(16) | 107.7(2) | C(36)−C(37)−C(38) | 106.3(2) |
| C(15)−C(16)−C(12) | 109.0(2) | C(37)−C(38)−C(34) | 108.8(2) |
| C(16)−C(12)−C(13) | 106.8(2) | C(38)−C(34)−C(35) | 107.8(2) |
| average C−C−C | 108 | average C−C−C | 108 |
| C(6)−C(5)−Cp(cent)(1) | 178.4 | C(27)−C(28)−Cp(cent)(3) | 179.5 |
| C(17)−C(16)−Cp(cent)(2) | 176.9 | C(38)−C(39)−Cp(cent)(4) | 178.6 |

[a] Cp(cent)(1)−Cp(cent)(4) denote centroids of the $C_5$ rings C(1)−C(5), C(12)−C(16), C(23)−C(27), and C(34)−C(38) respectively.

asymmetric unit of **8** is shown in Figure 2c (other figures shown in the Supporting Information). The C(23)−H(23)···$Cp_{Cent}$ distance of 2.617 Å and bond angle of 153° are typical for a C($sp^2$)−H donor and $\pi$ cloud acceptor.[23] It has been noted by Desiraju and Steiner[23] that the entire face of the aromatic ring can serve as a hydrogen bond acceptor, and this seems to be the case for **5**, where the C(23)−H(23)···$\pi$ is more closely positioned toward C(29) and C(40). Comparisons can be made between amino-functionalized ferrocene **5** and a different type of ferrocinium derivative, $[(FeC_5H_4CH_2NC_5H_5)]^{2+}\cdot 2[Br^-]$, which has recently been reported by Mingos et al.[8] They report short intermolecular Cp−H···$\pi$ interactions, but the situation is different in that they have observed interactions of one of the *ortho* Cp hydrogen atoms of one Cp of one molecule with the $\pi$ clouds of the pyridyl rings of the next to give distances of 2.82 and 2.88 Å and angles of 152° and 138°, respectively.[8] A Platon analysis was carried out on **3** and **4**, and this showed no intermolecular interactions of significance.

**Ferrocene Salt Compounds**. Finding suitable X-ray-quality crystals of the methylated ferrocenes **6**, **7**, and **10** proved not to be possible; however, the crystal structures of **8**, **11**, and **12** were determined, and there are different hydrogen-bonding properties associated with each structure. The bond lengths and angles for **8** are shown in Table 4. There are 1.5 molecules per asymmetric unit which prove to be quite different from each other with respect to the positioning of the substituted Cp rings. Both of the ring conformations and positioning of the pendant groups are different from those observed for the neutral ferrocene precursor **3**. For molecule 1 the Cp rings are staggered and the piperidinyl side chains are trans to each other: this is similar to the conformation of compound **4**. Molecule 2 represents a different bonding situation where the Cp rings are eclipsed and the pendant arms are virtually eclipsed, and this is shown in Figure 3.

There are also hydrogen-bonding interactions associated with each N−H group of compound **8**, which effectively link the ammonium cationic fragment and the trifluoroacetate anionic fragment. The details are shown in Table 5. The three bond lengths and angles are, respectively, N9−H9···O39B−C39 = 2.718 Å and 173.7°, N20−H20···O35A−C35 = 2.701 Å and 177.8°, and N31−H31···O37B−C37 = 2.723 Å and 168.2°; these are typical of N−H···O hydrogen bonds.

(23) Desiraju, G. R.; Steiner, T. *The Weak Hydrogen Bond*; Oxford Univerity Press: Oxford, 1999.

**Table 4.** Selected Interatomic Distances (Å) and Selected Angles (deg) between Interatomic Vectors with Estimated Standard Deviations in Parentheses for **8**[a]

| | | | |
|---|---|---|---|
| | Molecule 1 | | |
| Fe(1)−C(1) | 2.0809(19) | N(9)−C(9) | 1.492(2) |
| Fe(1)−C(2) | 2.057(2) | C(10)−C(11) | 1.521(3) |
| Fe(1)−C(3) | 2.056(2) | O(39a)−C(39) | 1.232(3) |
| Fe(1)−C(4) | 2.0543(19) | O(39b)−C(39) | 1.247(3) |
| Fe(1)−C(5) | 2.0561(19) | C(40)−F(40a) | 1.303(3) |
| C(1)−C(5) | 1.424(3) | C(40)−F(40b) | 1.335(3) |
| C(1)−C(6) | 1.508(3) | C(40)−F(40c) | 1.311(3) |
| C(3)−C(4) | 1.417(3) | C(39)−C(40) | 1.541(3) |
| C(6)−C(11) | 1.529(3) | Fe(1)−Cp(cent)(1) | 1.668 |
| C(7)−C(8) | 1.520(3) | | |
| C(5)−C(1)−C(2) | 106.92(17) | C(4)−C(5)−C(1) | 108.70(18) |
| C(4)−C(3)−C(2) | 107.79(18) | O(39b)−C(39)−C(40) | 114.7(2) |
| C(3)−C(2)−C(1) | 108.55(18) | O(39a)−C(39)−C(40) | 115.7(2) |
| C(3)−C(4)−C(5) | 108.03(18) | O(39a)−C(39)−O(39b) | 129.6(2) |
| | Molecule 2 | | |
| Fe(2)−Cp(cent)(2) | 1.661 | Fe(3)−Cp(cent)(3) | 1.655 |
| Fe(2)−C(25) | 2.0425(19) | Fe(2)−C(15) | 2.0492(19) |
| Fe(2)−C(26) | 2.052(2) | Fe(2)−C(24) | 2.0537(18) |
| Fe(2)−C(27) | 2.0569(19) | Fe(2)−C(16) | 2.0579(19) |
| Fe(2)−C(13) | 2.058(2) | Fe(2)−C(23) | 2.0620(18) |
| Fe(2)−C(12) | 2.0763(19) | C(12)−C(13) | 1.425(3) |
| C(12)−C(16) | 1.433(3) | C(12)−C(17) | 1.504(3) |
| C(13)−C(14) | 1.420(3) | C(14)−C(15) | 1.424(3) |
| C(15)−C(16) | 1.423(3) | C(17)−C(18) | 1.528(3) |
| C(17)−C(22) | 1.534(3) | C(18)−C(19) | 1.515(3) |
| C(19)−N(20) | 1.498(3) | N(20)−C(20) | 1.488(3) |
| N(20)−C(21) | 1.493(3) | C(21)−C(22) | 1.521(3) |
| C(23)−C(24) | 1.434(3) | C(23)−C(27) | 1.435(3) |
| C(23)−C(28) | 1.511(3) | C(24)−C(25) | 1.429(3) |
| C(25)−C(26) | 1.426(3) | C(26)−C(27) | 1.423(3) |
| C(28)−C(29) | 1.529(2) | C(28)−C(33) | 1.538(2) |
| C(29)−C(30) | 1.522(3) | C(30)−N(31) | 1.498(2) |
| N(31)−C(31) | 1.484(2) | N(31)−C(32) | 1.499(2) |
| C(32)−C(33) | 1.516(3) | C(35)−O(35b) | 1.224(3) |
| C(35)−O(35a) | 1.243(3) | C(35)−C(36) | 1.539(3) |
| C(36)−F(36c) | 1.309(3) | C(36)−F(36a) | 1.321(3) |
| C(36)−F(36b) | 1.326(3) | O(37a)−C(37) | 1.227(2) |
| O(37b)−C(37) | 1.250(2) | C(37)−C(38) | 1.547(3) |
| F(37a)−C(38) | 1.332(2) | F(37b)−C(38) | 1.341(2) |
| F(37c)−C(38) | 1.341(2) | | |
| C(13)−C(12)−C(16) | 107.15(17) | C(24)−C(23)−C(27) | 107.13(16) |
| C(14)−C(13)−C(12) | 108.59(18) | C(25)−C(24)−C(23) | 108.24(17) |
| C(16)−C(15)−C(14) | 107.74(18) | C(27)−C(26)−C(25) | 107.95(17) |
| C(15)−C(16)−C(12) | 108.42(18) | C(26)−C(27)−C(23) | 108.60(17) |
| C(13)−C(14)−C(15) | 108.09(18) | C(26)−C(25)−C(24) | 108.08(17) |
| O(35b)−C(35)−O(35a) | 128.8(2) | O(35b)−C(35)−C(36) | 116.20(19) |
| O(35a)−C(35)−C(36) | 114.98(18) | O(37a)−C(37)−O(37b) | 129.80(18) |
| O(37a)−C(37)−C(38) | 114.56(17) | O(37b)−C(37)−C(38) | 115.64(17) |

[a] Cp(cent)(1)−Cp(cent)(3) denote centroids of the $C_5$ rings C(1)−C(5), C(12)−C(16), and C(23)−C(27), respectively.

The bond lengths and angles for **11** are shown in Table 6. Even though they have the same counterion, $CF_3COO^-$, **11** differs from **8** considerably with respect to ring conformation and position of the pendant functional groups, presumably as a consequence of the different pendant arms. There is one molecule per asymmetric unit, which has a staggered ring conformation, as shown in Figure 4. The hydrogen-bonding situation is similar to that of **8**, with one N−H being bound to one $CF_3COO^-$ (bonds lengths and angles shown in Table 5). The bond lengths and angles for **12** are shown in Table 7. Changing the counterion $CF_3COO^-$ from compound **11** to $BF_4^-$ to form compound **12** has no effect on the disposition of the rings and substituents to each other, but presents a different hydrogen-bonding scenario. The molecular structure

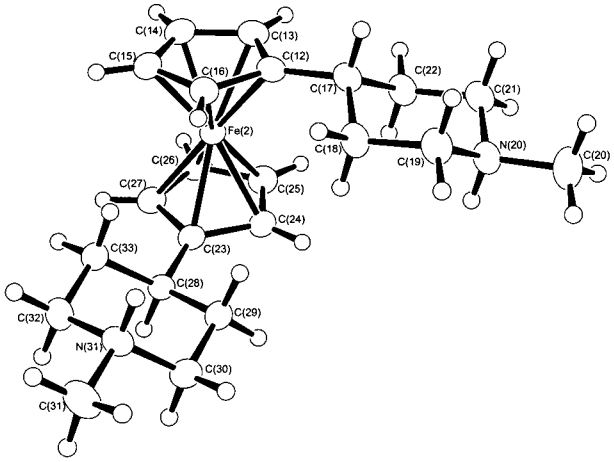


**Figure 3.** Molecular structure of molecule 2 from the asymmetric unit of **8**. The trifluoroacetate anions are omitted for clarity.

**Table 5.** Hydrogen Bond Distances and Angles for Compounds **8**, **11**−**13**, and **15**

| D−H | d(D−H) | d(H···A) | −DHA | d(D···A) | A |
|---|---|---|---|---|---|
| | | **8** | | | |
| N(9)−H(9) | 0.930 | 1.793 | 172.68 | 2.718 | O(39b) |
| N(20)−H(20) | 0.930 | 1.771 | 177.78 | 2.701 | O(35a) |
| N(31)−H(31) | 0.930 | 1.806 | 168.22 | 2.723 | O(37b) |
| | | **11** | | | |
| N(8)−H(8) | 1.0090 | 1.823 | 158.88 | 2.788 | O(101) |
| N(22)−H(22) | 1.0090 | 1.727 | 169.06 | 2.724 | O(200) |
| | | **12** | | | |
| N(8)−H(8) | 0.9305 | 2.024 | 153.37 | 2.886(3) | F(6) |
| N(8)−H(8) | 0.9305 | 2.263 | 143.99 | 3.065(3) | F(7) |
| N(28)−H(28) | 0.9307 | 2.051 | 155.08 | 2.922(3) | F(1) |
| N(28)−H(28) | 0.9307 | 2.225 | 142.19 | 3.015(3) | F(2) |
| | | **13** | | | |
| N(9)−H(9) | 0.929 | 1.925 | 164.23 | 2.831(14) | F(34) |
| N(20)−H(20) | 0.930 | 1.825 | 171.40 | 2.749(13) | F(33) |
| | | **15** | | | |
| N(8)−H(8) | 0.929 | 1.916 | 165.23 | 2.824(4) | F(6) |
| N(28)−H(28) | 0.9305 | 1.899 | 170.95 | 2.822(7) | F(8) |
| N(48)−H(48) | 0.9306 | 2.372 | 126.88 | 3.023(4) | F(2) |
| N(48)−H(48) | 0.9306 | 2.073 | 137.77 | 2.832(4) | F(16) |
| N(68)−H(68) | 0.9312 | 2.395 | 147.50 | 3.219(5) | F(9) |
| N(68)−H(68) | 0.9312 | 2.0121 | 143.80 | 2.818(5) | F(10) |

of **12** is shown in Figure 5. For **12**, there is one $BF_4^-$ counterion bound in an $\eta^2$ fashion (slightly asymmetric) to each N−H unit, and this is represented in Figure 5, the bond lengths and angles of which can be seen in Table 5.

**Ferrocenium Salt Compounds.** Oxidation of the Fe center to 3+ has the predicted effect of increasing the Fe to Cp(cent) distance by approximately 0.04 Å (1.66−1.70 Å). This is typical for oxidation of ferrocene to a ferrocenium compound. The bond lengths and angles for **13** are shown in Table 8. There is one molecule per asymmetric unit, and the two cyclopentadienyl rings are staggered with the pendant arms opposite each other.

There are two types of $BF_4^-$ counterions: (i) one $BF_4^-$ bound in a $C_2$-symmetric $\eta^2$ fashion to a N−H unit of two different molecules (on a 2-fold axis) as shown in Figure 6 and (ii) two unbound $BF_4^-$ counterions. The bond lengths and angles for **15** are shown in Table 9.

For **15** there is one molecule and two independent half-molecules per asymmetric unit, with the two half-molecules

**Table 6.** Selected Interatomic Distances (Å) and Selected Angles (deg) between Interatomic Vectors with Estimated Standard Deviations in Parentheses for **11**[a]

| | | | |
|---|---|---|---|
| C(1)−C(2) | 1.427(5) | C(1)−C(5) | 1.427(4) |
| C(1)−C(6) | 1.499(4) | C(1)−Fe(1) | 2.056(3) |
| C(2)−C(3) | 1.437(4) | C(2)−Fe(1) | 2.037(3) |
| C(3)−C(4) | 1.419(5) | C(3)−Fe(1) | 2.043(3) |
| C(4)−C(5) | 1.411(5) | C(4)−Fe(1) | 2.050(3) |
| C(5)−Fe(1) | 2.051(3) | C(6)−C(7) | 1.517(4) |
| C(15)−Fe(1) | 2.052(3) | C(16)−C(17) | 1.424(4) |
| C(16)−Fe(1) | 2.037(3) | C(17)−C(18) | 1.414(6) |
| C(17)−Fe(1) | 2.044(3) | C(18)−C(19) | 1.427(5) |
| C(18)−Fe(1) | 2.050(3) | C(19)−Fe(1) | 2.046(3) |
| C(100)−F(100) | 1.296(5) | C(100)−F(101) | 1.326(5) |
| C(100)−F(102) | 1.352(5) | C(100)−C(101) | 1.529(6) |
| C(101)−O(100) | 1.198(6) | C(101)−O(101) | 1.212(5) |
| C(200)−F(201) | 1.333(4) | C(200)−F(202) | 1.335(4) |
| C(200)−F(200) | 1.344(4) | C(200)−C(201) | 1.520(5) |
| C(201)−O(201) | 1.231(5) | C(201)−O(200) | 1.246(4) |
| Fe(1)−Cp(cent)(1) | 1.6502 | Fe(1)−Cp(cent)(2) | 1.6494 |
| C(2)−C(1)−C(5) | 106.7(3) | C(4)−C(5)−C(1) | 109.0(3) |
| C(1)−C(2)−C(3) | 108.7(3) | C(4)−C(3)−C(2) | 107.1(3) |
| C(5)−C(4)−C(3) | 108.5(3) | C(12)−C(11)−C(10) | 109.7(3) |
| C(19)−C(15)−C(16) | 107.6(3) | C(17)−C(16)−C(15) | 107.9(3) |
| C(17)−C(18)−C(19) | 107.7(3) | C(18)−C(17)−C(16) | 108.5(3) |
| O(100)−C(101)−O(101) | 128.6(5) | O(100)−C(101)−C(100) | 116.1(4) |
| O(101)−C(101)−C(100) | 115.1(4) | O(201)−C(201)−O(200) | 128.5(4) |
| O(201)−C(201)−C(200) | 116.9(3) | O(200)−C(201)−C(200) | 114.5(3) |
| Cp(cent)(1)−Fe(1)−Cp(cent)(2) | 179.00 | | |

[a] Cp(cent)(1) and Cp(cent)(2) denote centroids of the $C_5$ rings C(1)−C(5) and C(15)−C(19), respectively.

**Table 7.** Selected Interatomic Distances (Å) and Selected Angles (deg) between Interatomic Vectors with Estimated Standard Deviations in Parentheses for **12**[a]

| | | | |
|---|---|---|---|
| C(1)−C(2) | 1.416(4) | C(3)−C(4) | 1.428(4) |
| C(3)−C(2) | 1.413(4) | C(5)−C(4) | 1.429(4) |
| C(5)−C(1) | 1.413(4) | C(21)−C(22) | 1.420(4) |
| C(21)−C(25) | 1.428(4) | C(24)−C(23) | 1.414(4) |
| C(24)−C(25) | 1.425(4) | C(23)−C(22) | 1.417(4) |
| C(1)−Fe(1) | 2.050(3) | C(3)−Fe(1) | 2.049(3) |
| C(4)−Fe(1) | 2.051(3) | C(5)−Fe(1) | 2.056(2) |
| C(2)−Fe(1) | 2.046(3) | C(21)−Fe(1) | 2.053(3) |
| C(22)−Fe(1) | 2.040(3) | C(23)−Fe(1) | 2.049(3) |
| C(24)−Fe(1) | 2.052(3) | C(25)−Fe(1) | 2.057(2) |
| Fe(1)−Cp(cent)(1) | 1.6567 | Fe(1)−Cp(cent)(2) | 1.6562 |
| C(1)−C(5)−C(4) | 107.2(3) | C(23)−C(24)−C(25) | 108.5(3) |
| C(2)−C(3)−C(4) | 107.6(3) | C(3)−C(4)−C(5) | 108.2(3) |
| C(3)−C(2)−C(1) | 108.2(3) | C(22)−C(21)−C(25) | 107.9(3) |
| C(24)−C(23)−C(22) | 108.0(3) | C(24)−C(25)−C(21) | 107.3(2) |
| C(5)−C(1)−C(2) | 108.8(3) | C(23)−C(22)−C(21) | 108.3(3) |
| Cp(cent)(1)−Fe(1)−Cp(cent)(2) | 179.90 | | |

[a] Cp(cent)(1) and Cp(cent)(2) denote centroids of the $C_5$ rings C(1)−C(5) and C(21)−C(25), respectively.

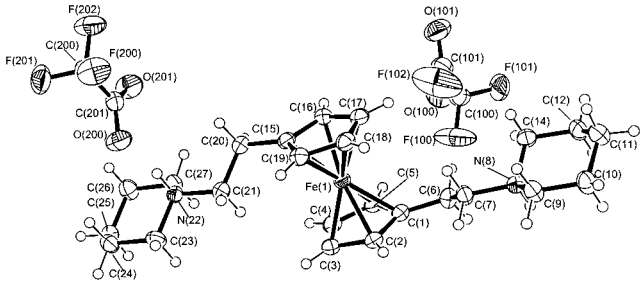


**Figure 4.** Molecular structure of compound **11**.

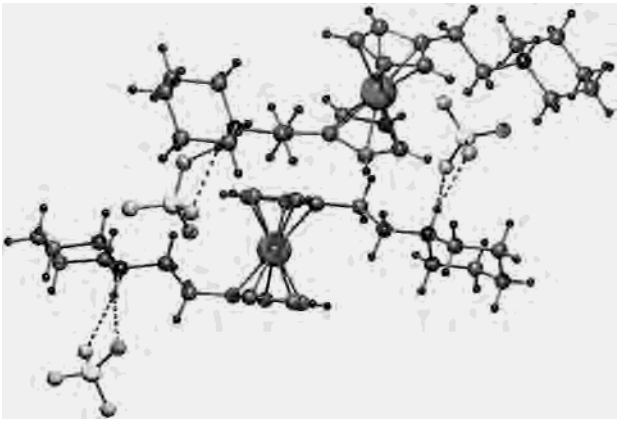

**Figure 5.** A diagram showing the hydrogen bonding involved with **12**.

on inversion centers of symmetry. The bond lengths and angles are shown in Table 9. Examination of the different types of hydrogen-bonding interactions (for bond lengths and angles, see Table 5) reveals intriguing patterns. The molecule without the inversion center of symmetry forms a hydrogen-bonded chain which is linked in an intermolecular fashion by $BF_4^-$ anions, which can be seen in Figure 7a. The molecules on the center of inversion have one N−H linked

**Table 8.** Selected Interatomic Distances (Å) and Selected Angles (deg) between Interatomic Vectors with Estimated Standard Deviations in Parentheses for **13**[a]

| | | | |
|---|---|---|---|
| C(1)−C(2) | 1.426(4) | C(3)−C(4) | 1.412(5) |
| C(2)−C(3) | 1.432(4) | C(1)−C(5) | 1.421(4) |
| C(4)−C(5) | 1.427(4) | Fe(1)−C(1) | 2.115(3) |
| Fe(1)−C(2) | 2.078(3) | Fe(1)−C(3) | 2.064(3) |
| Fe(1)−C(4) | 2.076(3) | Fe(1)−C(5) | 2.104(3) |
| Fe(1)−Cp(cent)(1) | 1.7003 | | |
| C(1)−C(2)−C(3) | 108.4(3) | C(2)−C(1)−C(5) | 107.1(3) |
| C(2)−C(3)−C(4) | 107.9(3) | C(5)−C(4)−C(3) | 107.8(3) |
| C(4)−C(5)−C(1) | 108.8(3) | | |

[a] Cp(cent)(1) and Cp(cent)(2) denote centroids of the $C_5$ rings C(1)−C(5) and C(12)−C(16), respectively.

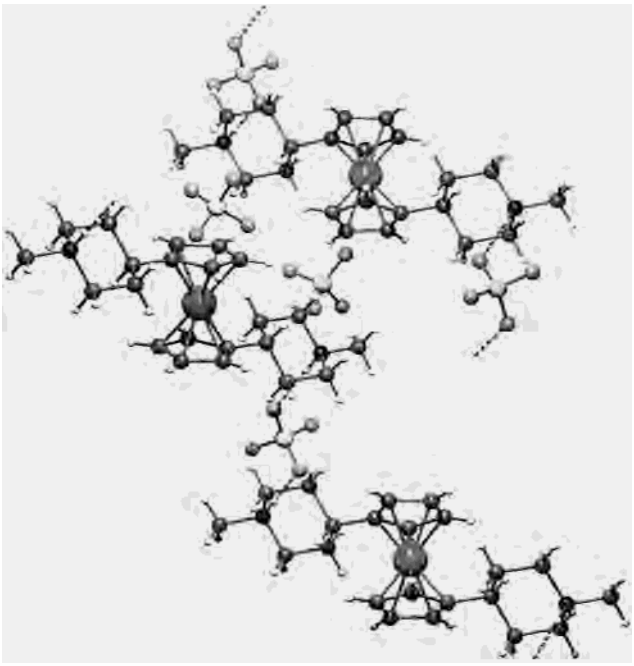

**Figure 6.** Unit cell of **13** showing the intermolecular hydrogen-bonding interactions.

to two different $BF_4^-$ anions and one $BF_4^-$ anion which is bound in an $\eta^2$ fashion to a N−H unit of one molecule (similar to **12**), and this is shown in Figure 7b. Two of the $BF_4^-$ counterions are unbound.

The electrochemistry of some of the compounds, **3**−**5**, **7**, and **8**, was examined, and their potentials are summarized in Table 10. All of the compounds exhibit a reversible oxidation process at approximately 0.00 V. Compared to the redox potential of the ferrocenium/ferrocene couple, this oxidation process can be assigned to the $Fe^{3+}/Fe^{2+}$ couple. Two additional reversible oxidation processes were observed at either side of the metal-based redox process for the ferrocene salts **7**−**10**, where iodide was used as counterion. These potentials were similar to those of sodium iodide (0.23 and 0.32 V) in the same electrolyte solution and can be assigned to the oxidation couples of the iodide counterion.

For the neutral ferrocene compounds **3**−**5**, a reversible oxidation process was followed by one or two broad and weak irreversible oxidation peaks at higher potentials. Scanning through these irreversible oxidation processes severely distorted the returning wave of the metal-based reversible couple. A similar distortion was also observed for

**Table 9.** Selected Interatomic Distances (Å) and Selected Angles (deg) between Interatomic Vectors with Estimated Standard Deviations in Parentheses for **15**[a]

| | | | |
|---|---|---|---|
| Fe(1)−C(2) | 2.050(3) | Fe(1)−C(3) | 2.065(4) |
| Fe(1)−C(22) | 2.073(3) | Fe(1)−C(21) | 2.078(3) |
| Fe(1)−C(1) | 2.089(3) | Fe(1)−C(23) | 2.093(3) |
| Fe(1)−C(25) | 2.097(3) | Fe(1)−C(24) | 2.106(3) |
| Fe(1)−C(4) | 2.108(3) | Fe(1)−C(5) | 2.138(3) |
| C(21)−C(22) | 1.414(5) | C(21)−C(25) | 1.436(5) |
| C(1)−C(2) | 1.424(5) | C(1)−C(5) | 1.434(5) |
| C(2)−C(3) | 1.413(6) | C(5)−C(4) | 1.426(5) |
| C(22)−C(23) | 1.417(5) | C(23)−C(24) | 1.409(5) |
| C(3)−C(4) | 1.422(5) | C(25)−C(24) | 1.426(5) |
| Fe(3)−C(44) | 2.071(4) | C(41)−C(42) | 1.419(6) |
| Fe(3)−C(43) | 2.072(4) | C(43)−C(42) | 1.381(7) |
| Fe(3)−C(42) | 2.082(4) | C(45)−C(44) | 1.411(5) |
| Fe(3)−C(41) | 2.096(4) | C(45)−C(41) | 1.414(5) |
| Fe(3)−C(45) | 2.101(3) | C(44)−C(43) | 1.417(7) |
| Fe(2)−C(63) | 2.068(3) | C(65)−C(61) | 1.428(5) |
| Fe(2)−C(62) | 2.073(3) | C(63)−C(62) | 1.420(5) |
| Fe(2)−C(64) | 2.093(3) | C(62)−C(61) | 1.440(5) |
| Fe(2)−C(61) | 2.100(3) | C(65)−C(64) | 1.429(5) |
| Fe(2)−C(65) | 2.139(3) | C(63)−C(64) | 1.418(5) |
| Fe(1)−Cp(cent)(1) | 1.7039 | Fe(2)−Cp(cent)(3) | 1.7060 |
| Fe(1)−Cp(cent)(2) | 1.7046 | Fe(3)−Cp(cent)(4) | 1.7081 |
| C(22)−C(21)−C(25) | 108.0(3) | C(4)−C(5)−C(1) | 107.3(3) |
| C(3)−C(2)−C(1) | 107.9(3) | C(24)−C(23)−C(22) | 108.2(3) |
| C(21)−C(22)−C(23) | 108.2(3) | C(3)−C(4)−C(5) | 108.0(3) |
| C(2)−C(3)−C(4) | 108.6(3) | C(24)−C(25)−C(21) | 107.0(3) |
| C(30)−C(31)−C(32) | 110.7(3) | C(23)−C(24)−C(25) | 108.5(3) |
| C(45)−C(44)−C(43) | 108.6(4) | C(44)−C(45)−C(41) | 107.1(3) |
| C(45)−C(41)−C(42) | 107.7(4) | C(42)−C(43)−C(44) | 107.8(4) |
| C(43)−C(42)−C(41) | 108.8(4) | C(63)−C(64)−C(65) | 109.0(3) |
| C(61)−C(65)−C(64) | 107.0(3) | C(65)−C(61)−C(62) | 108.3(3) |
| C(64)−C(63)−C(62) | 108.1(3) | C(63)−C(62)−C(61) | 107.6(3) |

[a] Cp(cent)(1)−Cp(cent)(4) denote centroids of the $C_5$ rings C(1)−C(5), C(21)−C(25), C(41)−C(45), and C(61)−C(65), respectively.

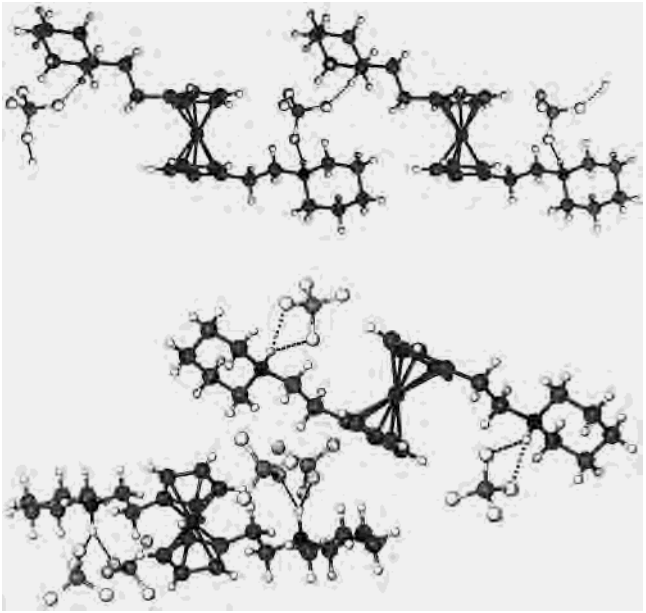

**Figure 7.** (a, top) A representation of the hydrogen bonding in **15** of the molecule without inversion symmetry. (b, bottom) A representation of the hydrogen-bonding pattern of **15** of the two molecules with inversion symmetry.

ferrocenophane derivatives by Osakada and co-workers.[24] However, if the scanning potential excludes the irreversible

(24) Sakano, T.; Ishii, H.; Yamaguchi, I.; Osakado, K.; Yamamoto, T. *Inorg. Chim. Acta* **1999**, *296*, 176.

**Table 10.** Redox Potentials of Compounds **3**−**5**, **7**, and **8**

| compd | potential | | |
|---|---|---|---|
| **3** | −0.08 | 0.57[b] | 1.20[b] |
| **4** | −0.10 | 0.57[b] | |
| **5** | −0.04 | 0.53[b] | |
| **7** | −0.18 | 0.05 | 0.26 |
| **8** | 0.00 | 0.72[b] | |
| **10** | **−0.15** | 0.08 | 0.25 |

[a] The potentials of compounds **10**−**12** were collected in 0.5 M $[N^nBu_4][BF_4]/CH_2Cl_2$ and the others in 0.1 M $[N^nBu_4][BF_4]/CH_3CN$. [b] Irreversible oxidation processes and hence anodic peak potentials were quoted.

oxidation processes, a fully reversible redox process is restored. The observation reveals that there was no chemical reaction following the metal-based redox process as suggested by Osakada.[24] It is possible that the first irreversible oxidation was due to the direct oxidation of the nitrogen atom on the pendant arm, and the decomposition of its oxidized product may give the second irreversible peak.

In the case of compound **8**, besides the reversible oxidation expected, a small irreversible peak was observed, but different from **3** and **4**, its existence had no influence on the metal-based oxidation. In general it was observed that the positively charged ferrocene salts **7** and **8** shift the oxidation potentials in a positive direction.

In conclusion, in this paper we report a number of novel 1,1′-bis-amino-functionalized ferrocenes and their ferrocene salt and ferrocenium salt counterparts. Electrochemical and structural studies have been carried out showing a number of interesting features, including electrostatic and hydrogen bond interactions for all classes of compounds, such as C−H···N and C−H···$\pi$ cloud interactions as well as N−H···O and N−H···F hydrogen bonds. Also included are the first crystallographically characterized examples of cyclopentadienyl units containing (piperidin-*N*-ylethyl)- and (pyrid-2-ylmethyl)cyclopentadienyl side chains.

**Acknowledgment.** We thank Dr. M. A. Halcrow for helpful comments and the EPSRC for funding.

**Supporting Information Available:** Additional figures consisting of unit cell contents and C−H···$\pi$ and H-bonding interactions for compounds **5**, **8, 12**, and **13** and the molecular structures of **12**, **13**, and **15** and crystallographic data in CIF format. This material is available free of charge via the Internet at http://pubs.acs.org.

IC010821K